Electronic Supplementary Material (ESI) for Polymer Chemistry.
This journal is © The Royal Society of Chemistry 2020

Supporting Information

Functionalisation and stabilisation of polymeric arsenical nanoparticles prepared by sequential reductive and radical cross-linking

*Joji Tanaka[‡,f], Alexander Evans[‡], Pratik Gurnani[†], Andrew Kerr, Paul Wilson**

University of Warwick, Department of Chemistry, Coventry, CV4 7AL, UK

SUPPLEMENTARY TABLES & FIGURES

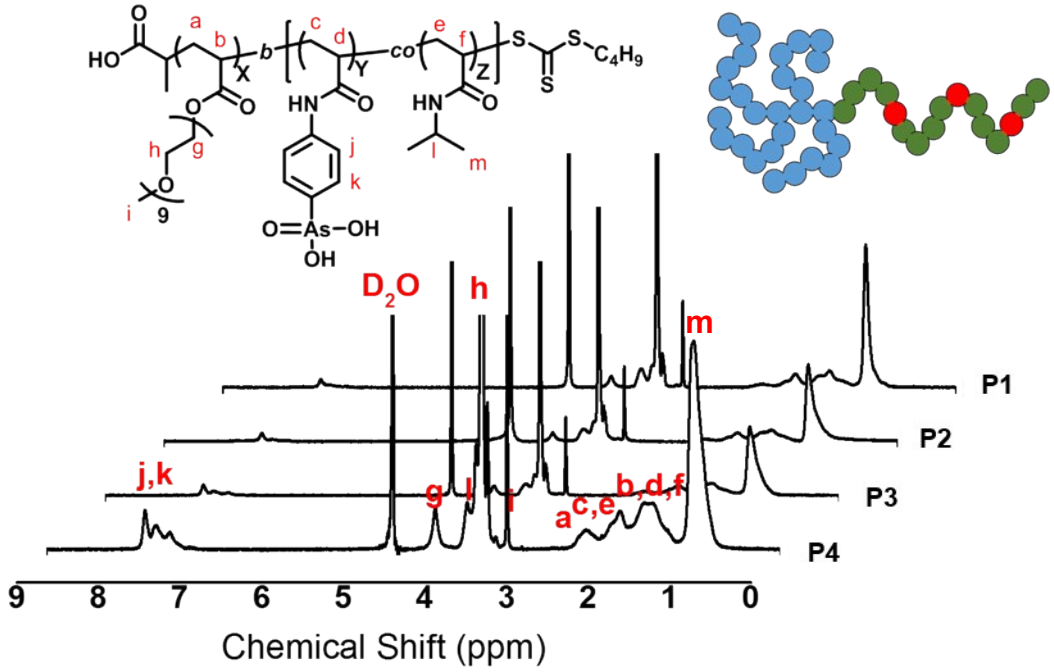

Fig. S1. ^{1}H NMR (D_2O) of the final polymer **P1** - **P4**

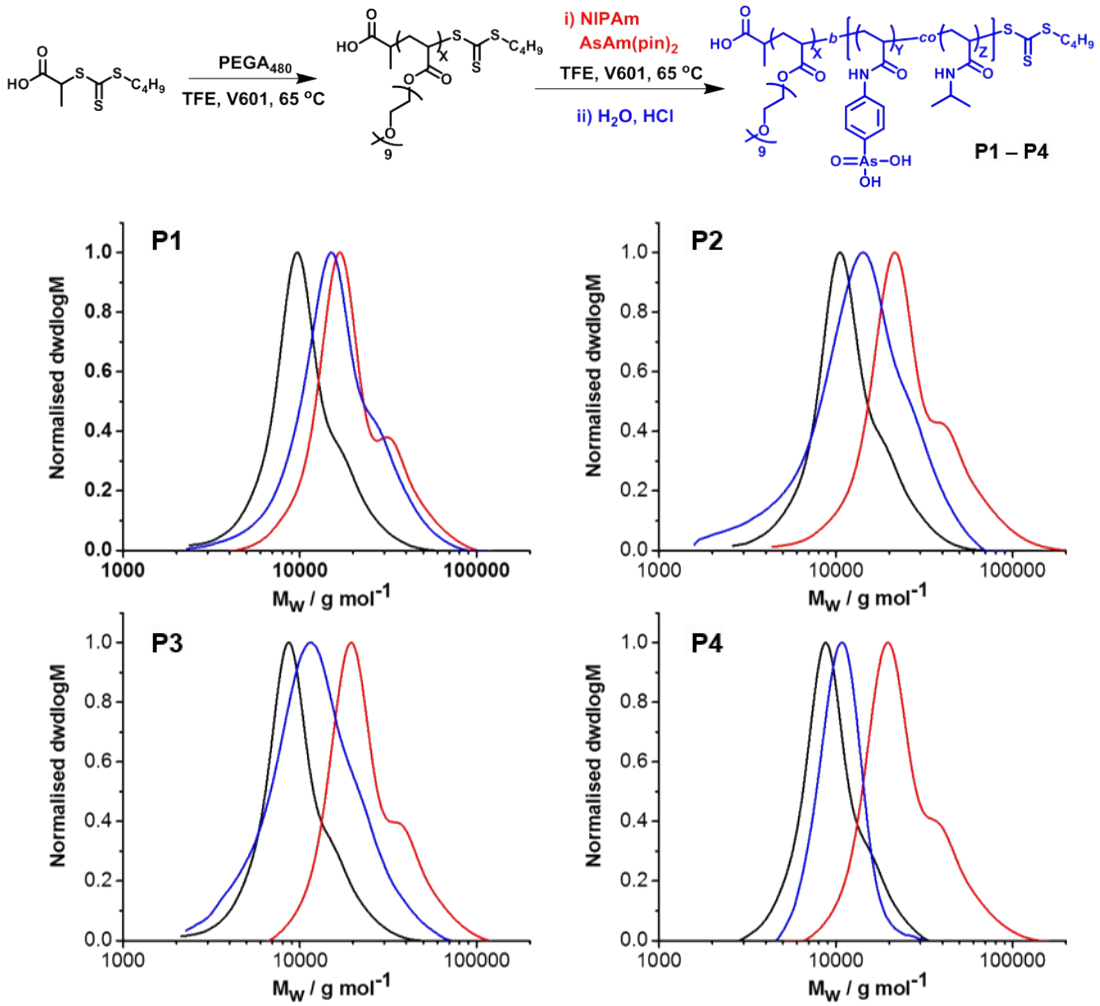

Fig. S2. SEC (DMF) of the arsenic functional block copolymers **P1** – **P4** showing the first block (black), chain extension extension (red) and removing the pinacol groups (blue).

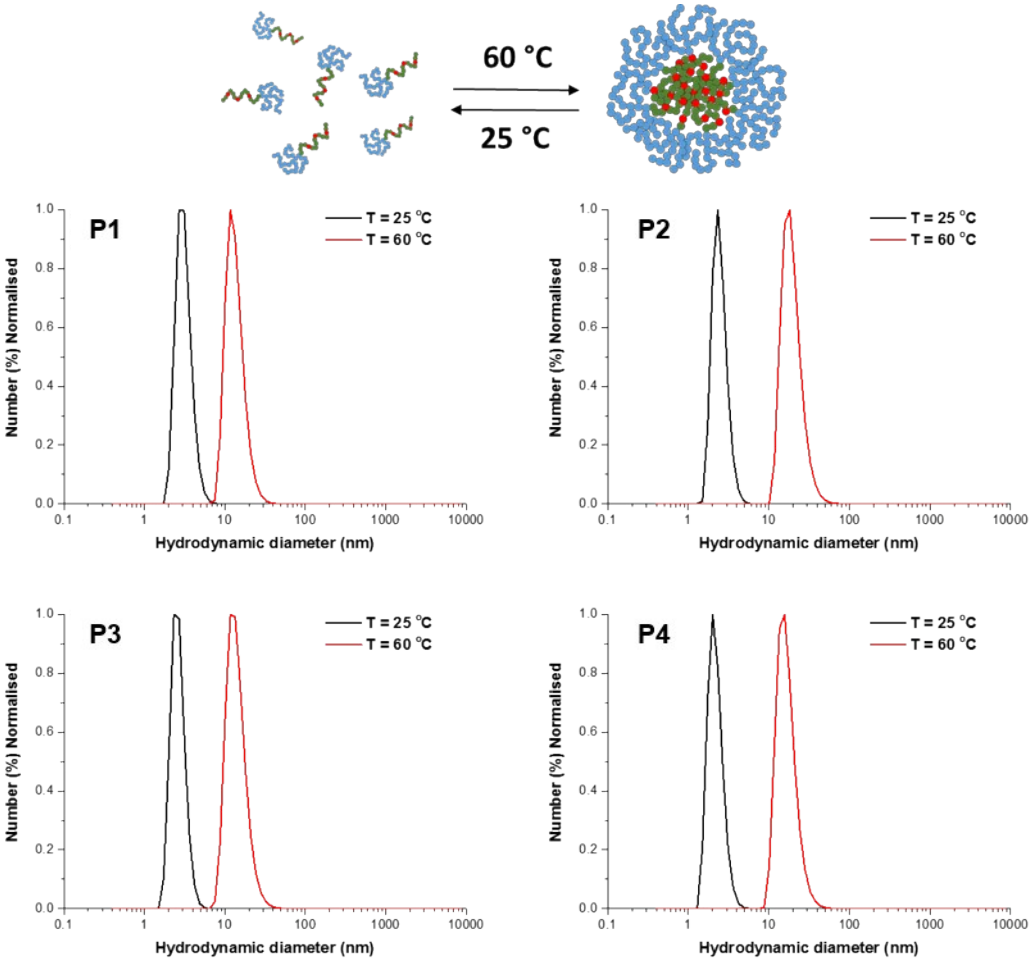

Fig. S3. Particle size distribution curves of **P1** – **P4** by dynamic light scattering (1 mg/mL, H_2O) analysis at 25 °C and 60 °C

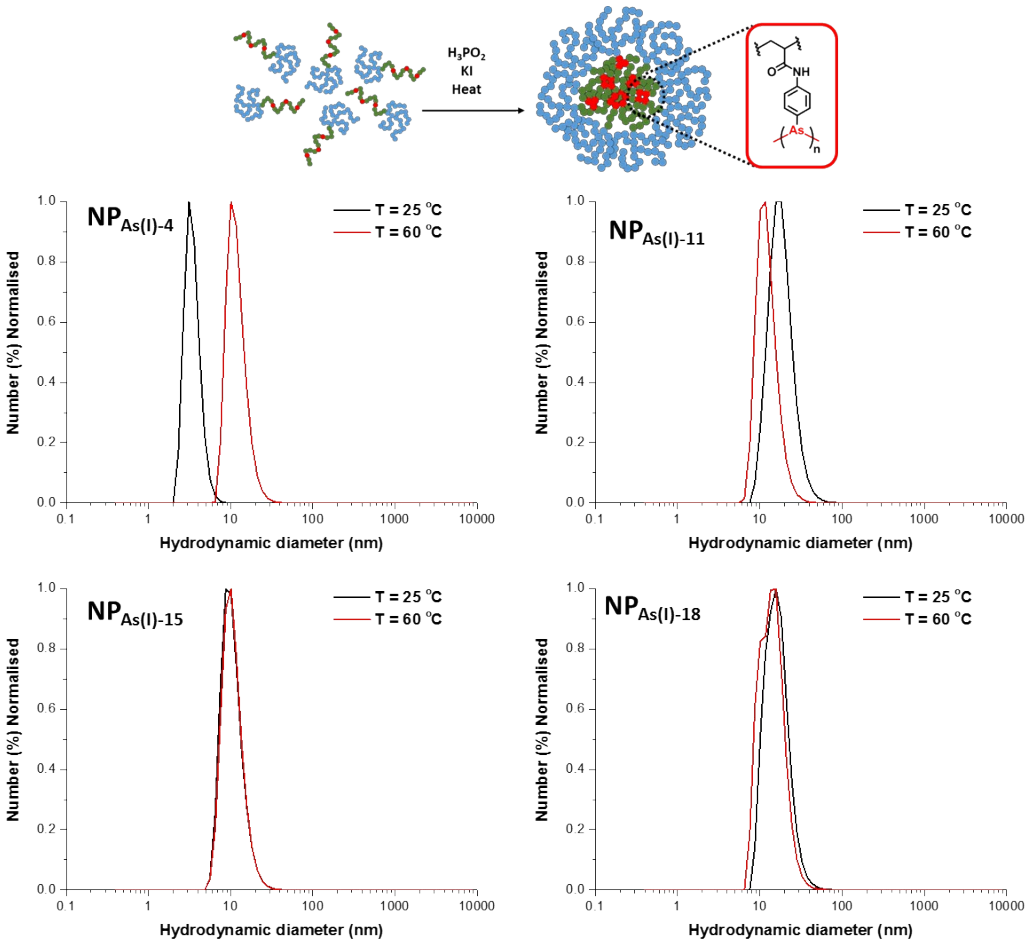

Fig. S4. Particle size distribution curves of **$NP_{As(I)-n}$** (n = 4, 11, 15, 18) by DLS (1 mg/mL, H_2O) analysis at 25 °C and 60 °C

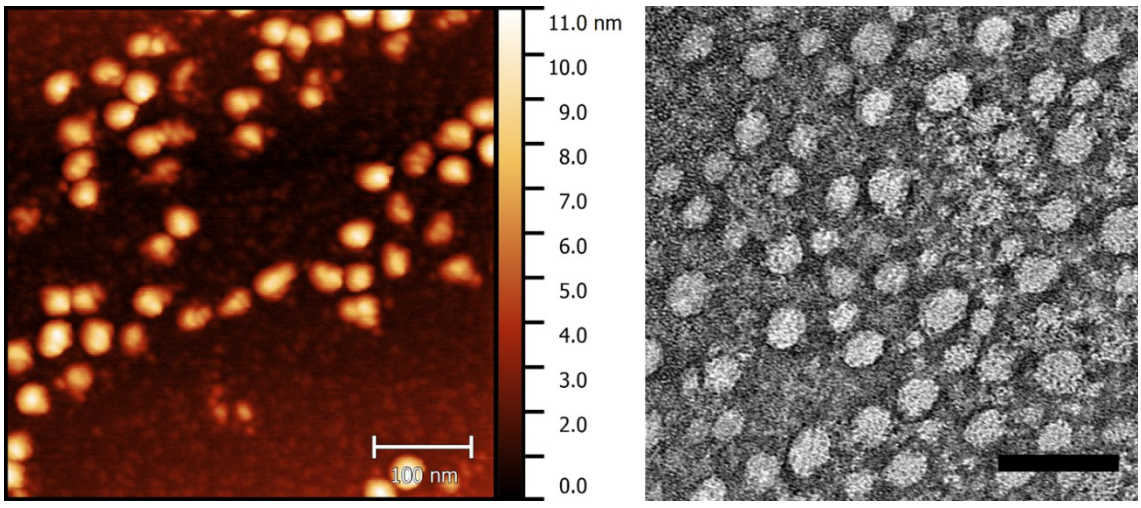

Fig. S5. AFM (left) and TEM (right) of **$NP_{As(I)-18}$** (scale bar = 100 nm)

Table S1. Particle size of $\mathbf{NP_{PgOH-n}}$ by dynamic light scattering at 25 °C and 60 °C in aqueous solution (1 mg/mL) (PDI calculated using Eq 1)

		25 °C		60 °C	
		D_h (nm)	PDi	D_h (nm)	PDI
P1	Polymer	3.12	0.052	13.60	0.077
	$\mathbf{NP_{PgOH-4}}$	11.3	0.108	9.47	0.101
P2	Polymer	2.47	0.046	19.7	0.097
	$\mathbf{NP_{PgOH-11}}$	12.7	0.095	14.0	0.119
P3	Polymer	2.65	0.043	14.2	0.093
	$\mathbf{NP_{PgOH-15}}$	14.1	0.106	140	0.119
P4	Polymer	2.20	0.050	16.9	0.090
	$\mathbf{NP_{PgOH-18}}$	15.1	0.099	13.5	0.107

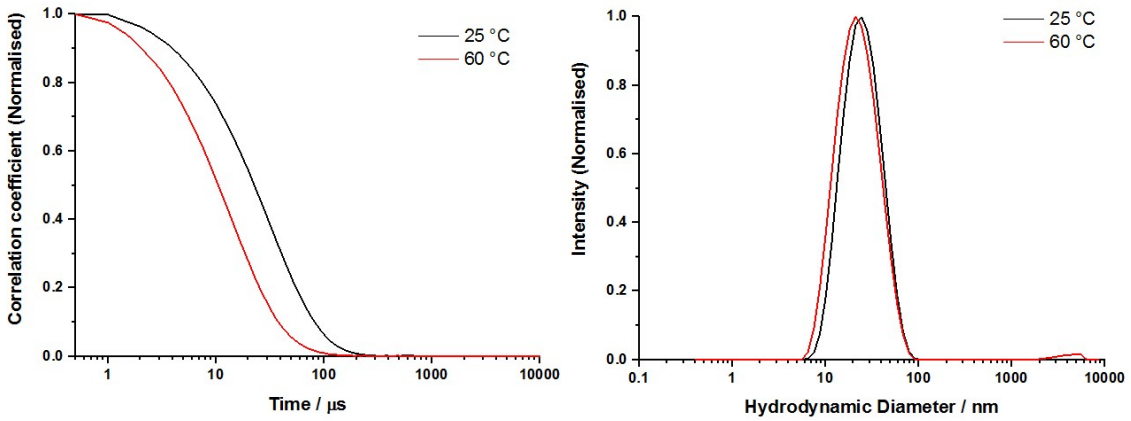

Fig S6A: DLS Correlation coefficient and intensity distribution for NP_{PgOH-4} as function of temperature

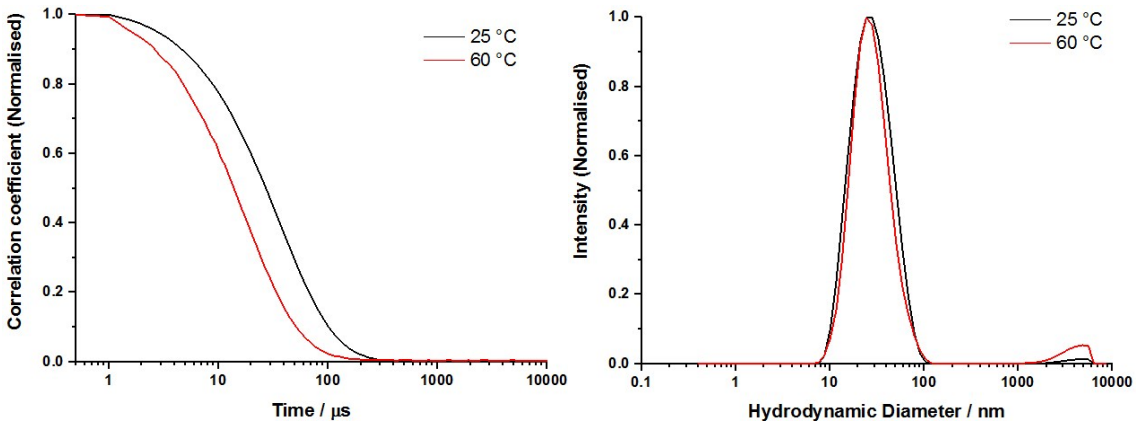

Fig S6B: DLS Correlation coefficient and intensity distribution for $NP_{PgOH-11}$ as function of temperature

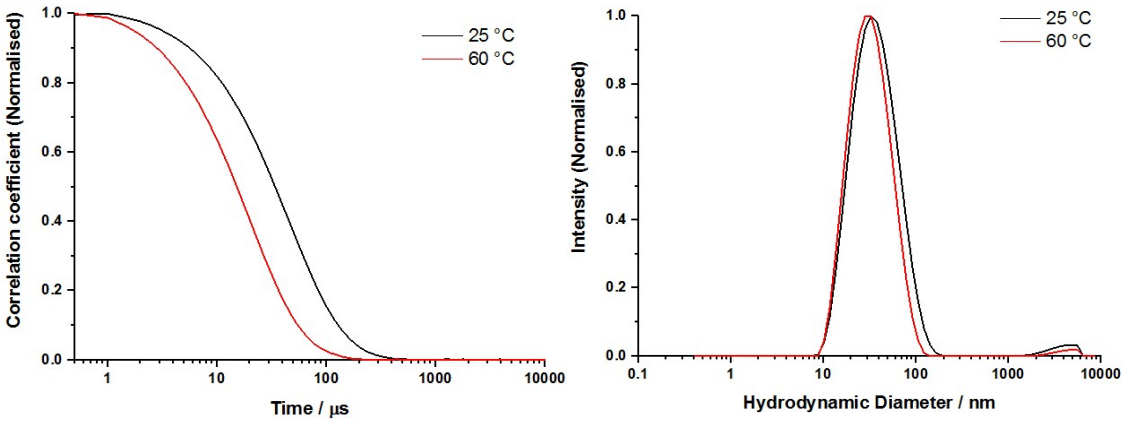

Fig S6C: DLS Correlation coefficient and intensity distribution for $NP_{PgOH-15}$ as function of temperature

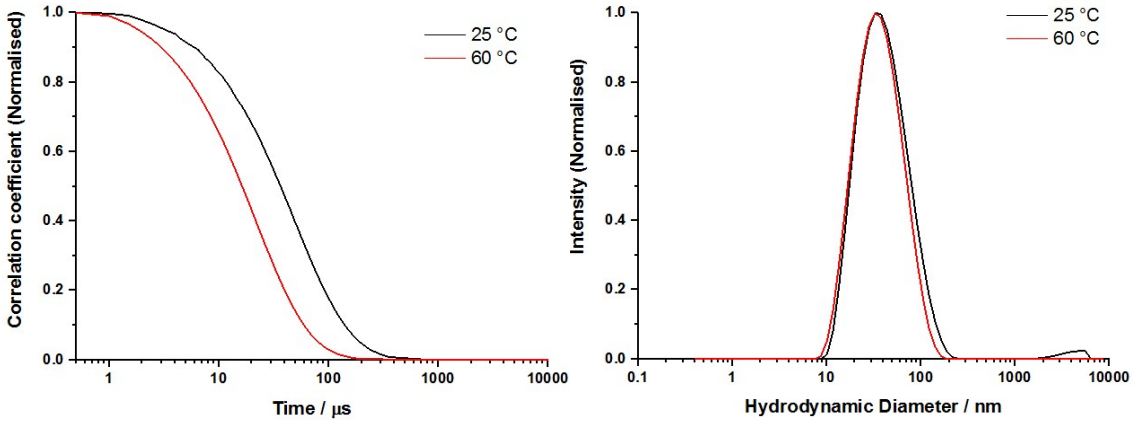

Fig. S6D: DLS Correlation coefficient and intensity distribution for $NP_{PgOH-18}$ as function of temperature

Table S2. Particle size of $\mathbf{NP_{PgNH-n}}$ and $\mathbf{NP_{PgAc-n}}$ by dynamic light scattering at 25 °C and 60 °C in aqueous solution (1 mg/mL) (PDI calculated using Eq 1)

		25 °C		60 °C	
		D_h (nm)	PDi	D_h (nm)	PDi
P2	$\mathbf{NP_{PgNH-11}}$	30.9	0.138	28.2	0.126
	$\mathbf{NP_{PgAc-11}}$	17.6	0.014	20.3	0.102
P3	$\mathbf{NP_{PgNH-15}}$	24.9	0.122	23.5	0.142
	$\mathbf{NP_{PgAc-15}}$	21.5	0.108	22.5	0.110
P4	$\mathbf{NP_{PgNH-18}}$	23.5	0.022	23.5	0.143

$NP_{PgAc-18}$	21.8	0.090	20.5	0.098

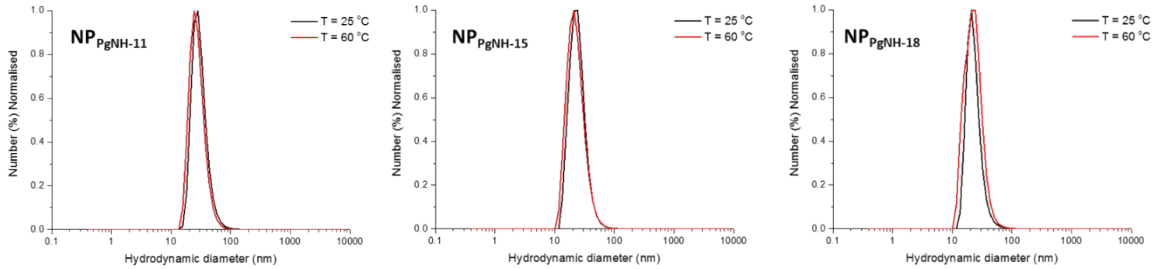

Fig. S7. Particle size distribution curves of **NP_{PAc-n}** (n = 11, 15, 18) by dynamic light scattering (1 mg/mL, H_2O) analysis at 25 °C and 60 °C.

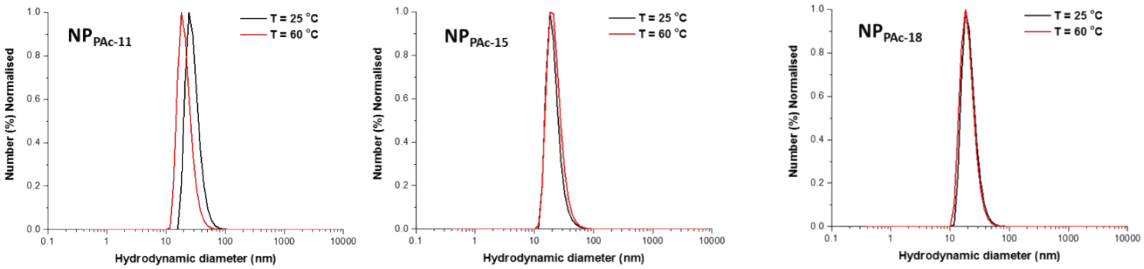

Fig. S8. Particle size distribution curves of **NP_{PAc-n}** (n = 11, 15, 18) by dynamic light scattering (1 mg/mL, H_2O) analysis at 25 °C and 60 °C.

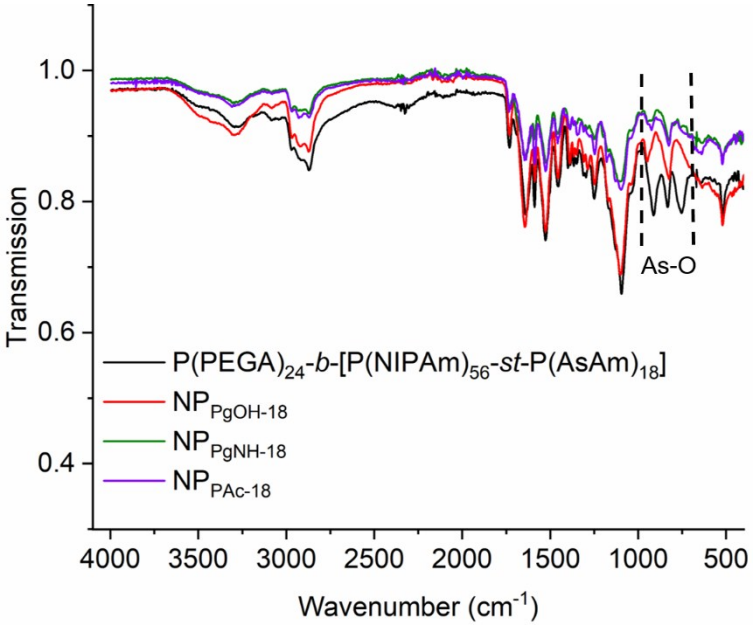

Fig. S9. Infrared spectra of **P4** (black), **NP$_{PgOH-18}$** (red), **NP$_{PgNH-18}$** (green) and **NP$_{PAc-18}$** (purple) indicating reduction and modification of the pendent arsenic acid (As(V)) groups via changes in the As-O region.

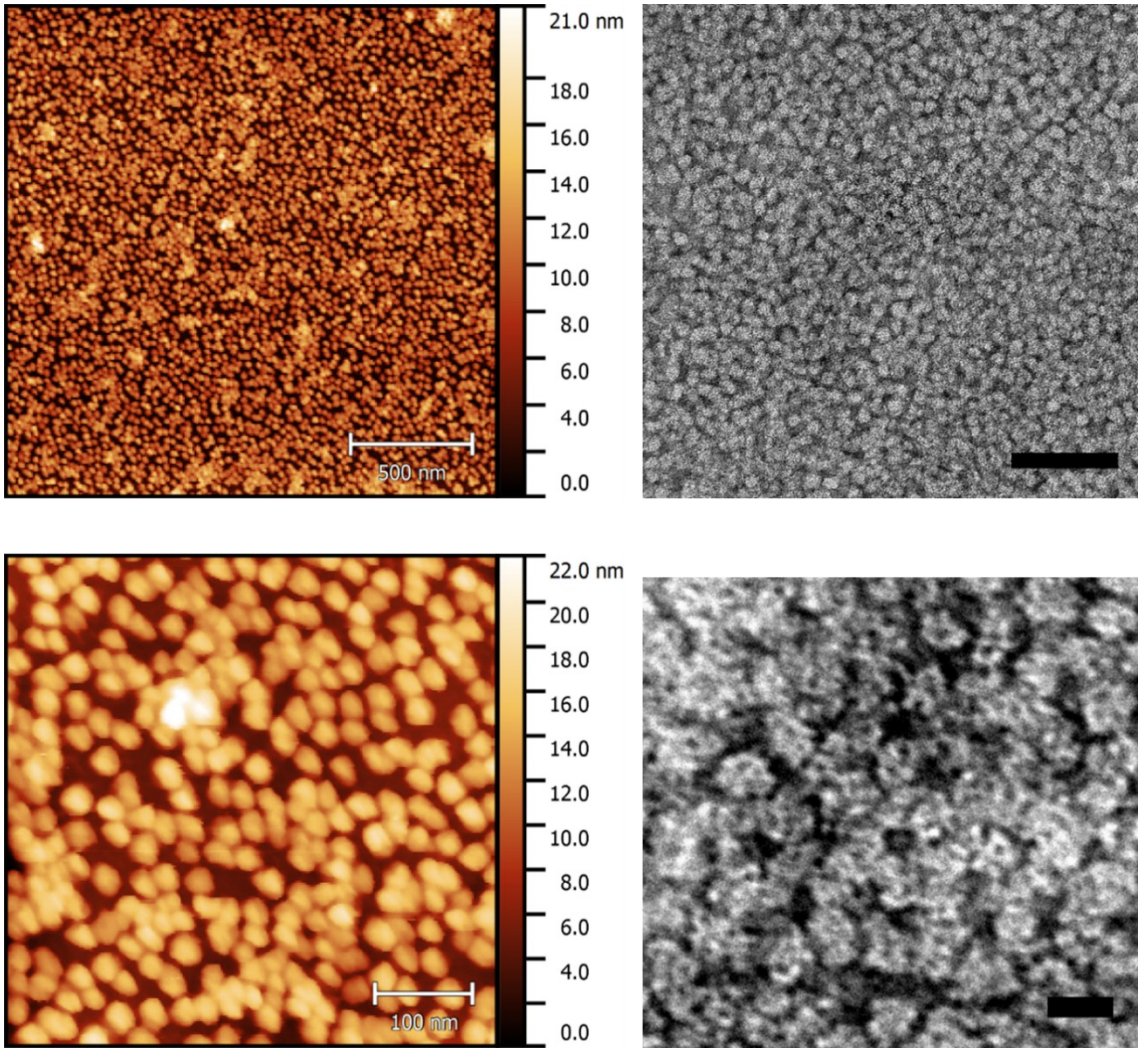

Fig. S10. AFM (left) and TEM (right) of $\mathbf{NP_{PgNH\text{-}18}}$ (bottom row scale bar = 100 nm, top row scale bar = 500 nm)

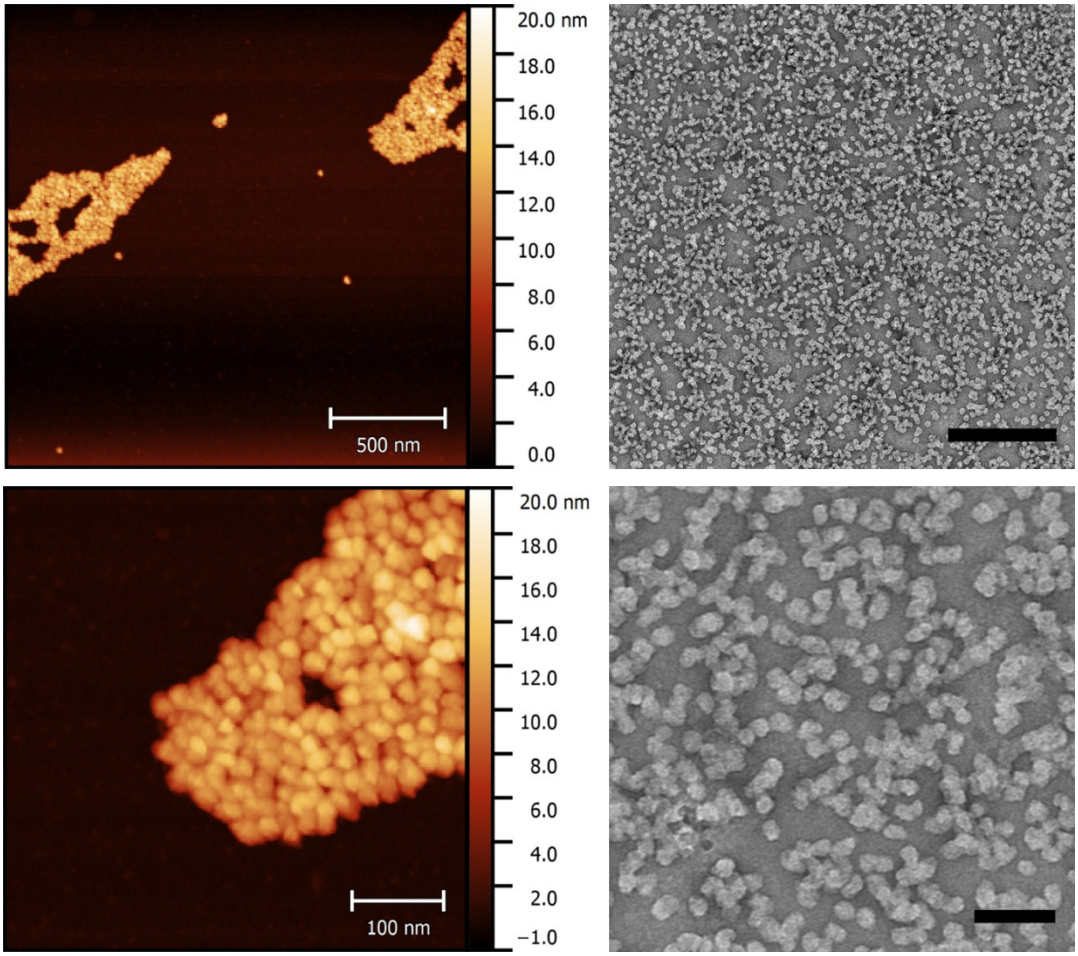

Fig. S11. AFM (left) and TEM (right) of $\mathbf{NP_{PAc\text{-}18}}$ (bottom row scale bar = 100 nm, top row scale bar = 500 nm)

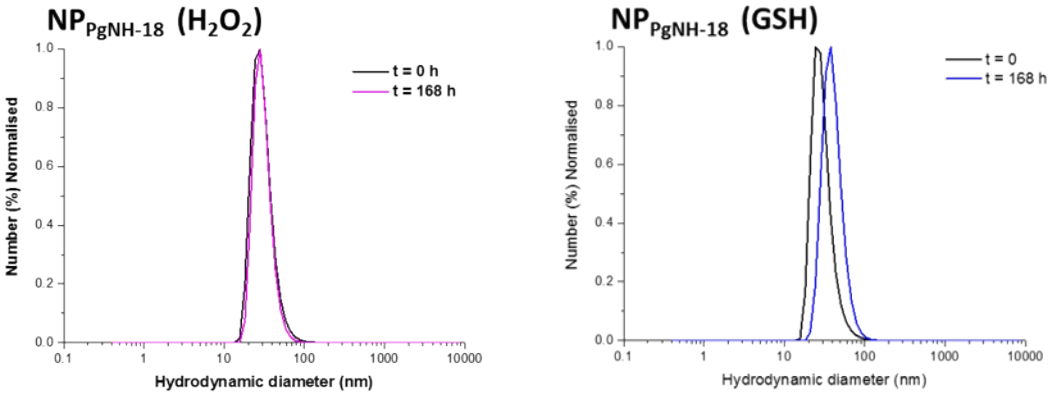

Fig. S12. Particle size distribution curves of **$NP_{PgNH-18}$** by dynamic light scattering (1 mg/mL) as function of time in aqueous H_2O_2 (5mM, left) and GSH (5mM, right)

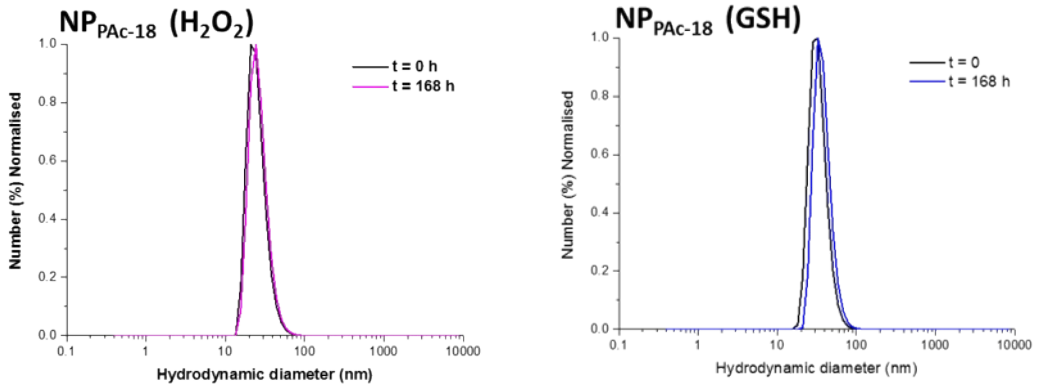

Fig. S13. Particle size distribution curves of **NP_{PAc-18}** by dynamic light scattering (1 mg/mL) as function of time in aqueous H_2O_2 (5mM, left) and GSH (5mM, right)

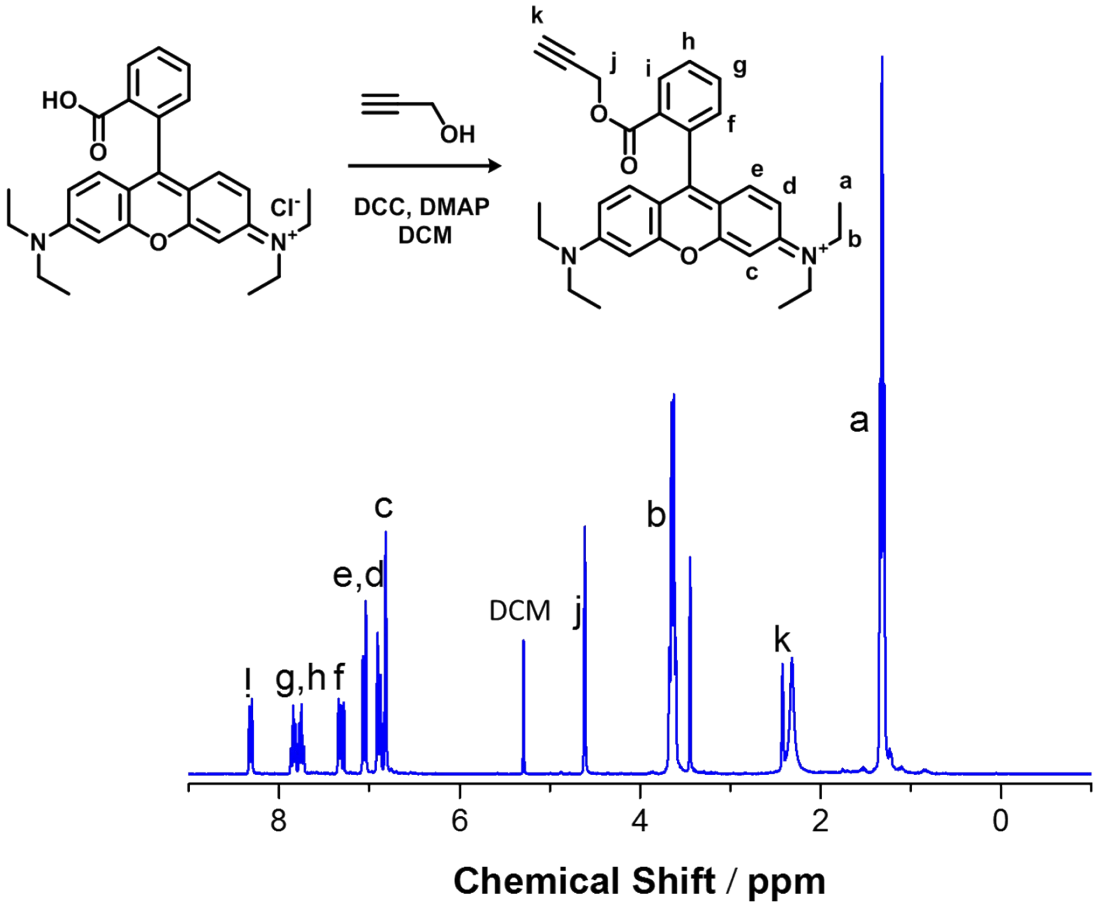

Fig. S14. Reaction scheme and ^{1}H-NMR spectrum for the synthesis of propargyl-*O*-rhodamine-B ester

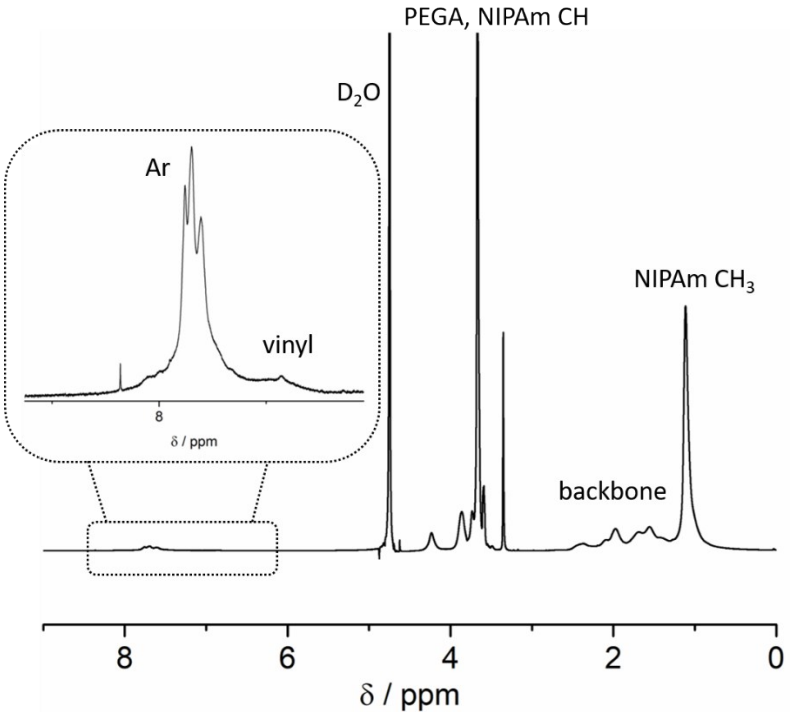

Fig. S15A. ^{1}H-NMR (D_2O) of $NP_{Rh\text{-}18}$ (100 mg/mL) showing obscured vinyl proton at 6.86 ppm.

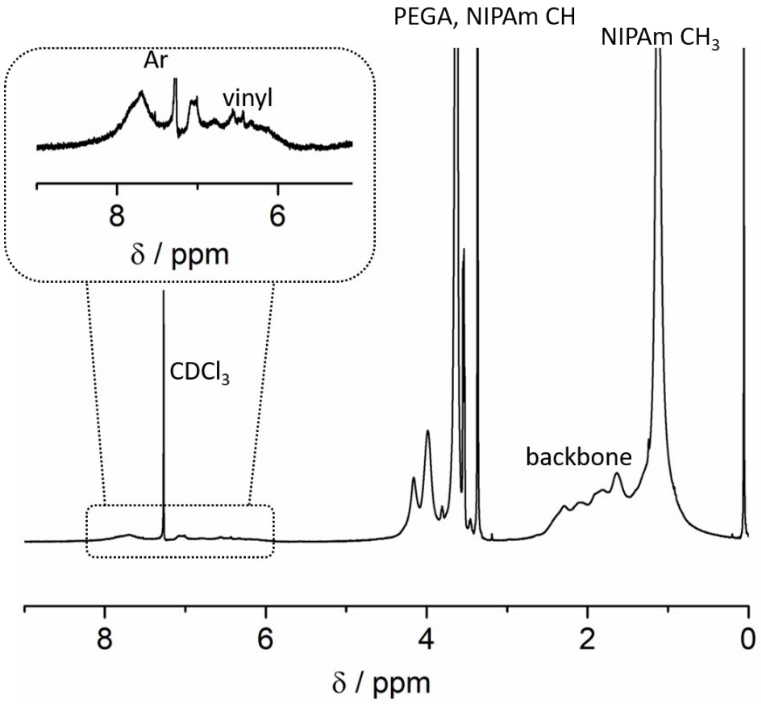

Fig. S15B. ^{1}H-NMR ($CDCl_3$) of $NP_{Rh\text{-}18}$ (100 mg/mL) showing obscured vinyl proton at 6.54 ppm.

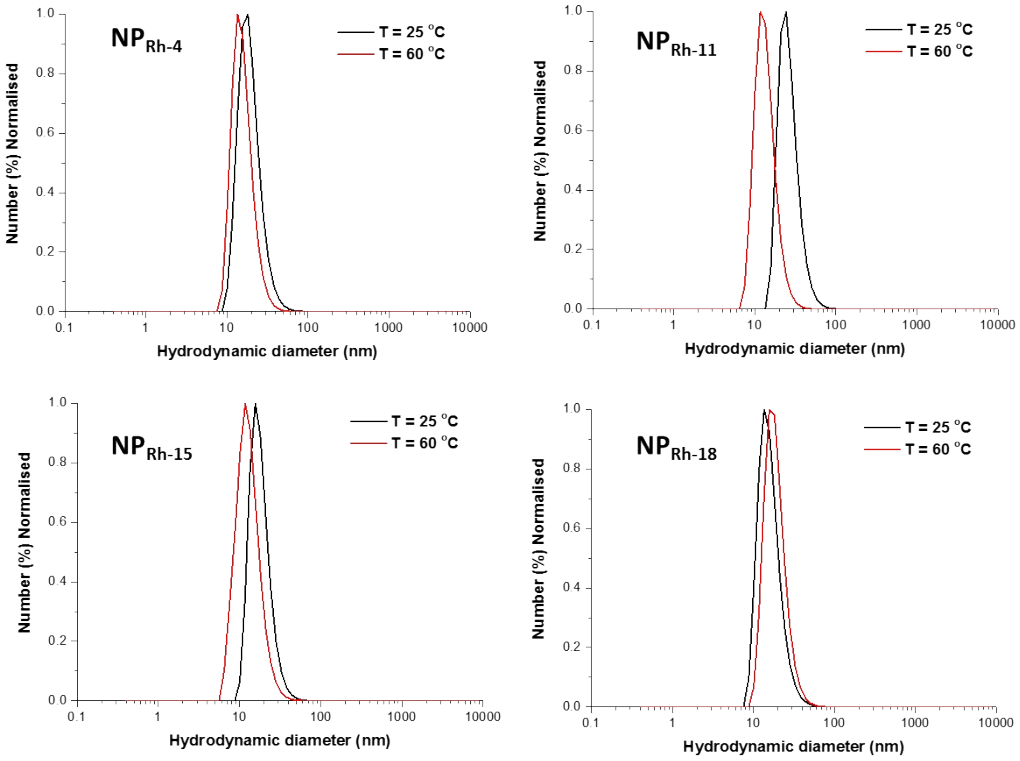

Fig. S16. Particle size distribution curves of $\mathbf{NP_{Rh\text{-}n}}$ (n = 4, 11, 15, 18) by dynamic light scattering (1 mg/ml, H_2O) analysis at 25 °C and 60 °C.

Table S3. Particle size of $\mathbf{NP_{Rh\text{-}n}}$ by dynamic light scattering at 25 °C and 60 °C in aqueous solution (1 mg/mL) (PDI calculated using Eq 1)

		25 °C		60 °C	
		D_h (nm)	PDi	D_h (nm)	PDi
P1	$\mathbf{NP_{Rh\text{-}4}}$	19.6	0.129	16.0	0.102
P2	$\mathbf{NP_{Rh\text{-}11}}$	26.7	0.098	13.8	0.099
P3	$\mathbf{NP_{Rh\text{-}15}}$	18.3	0.102	13.8	0.099
P4	$\mathbf{NP_{Rh\text{-}18}}$	16.3	0.131	19.0	0.113

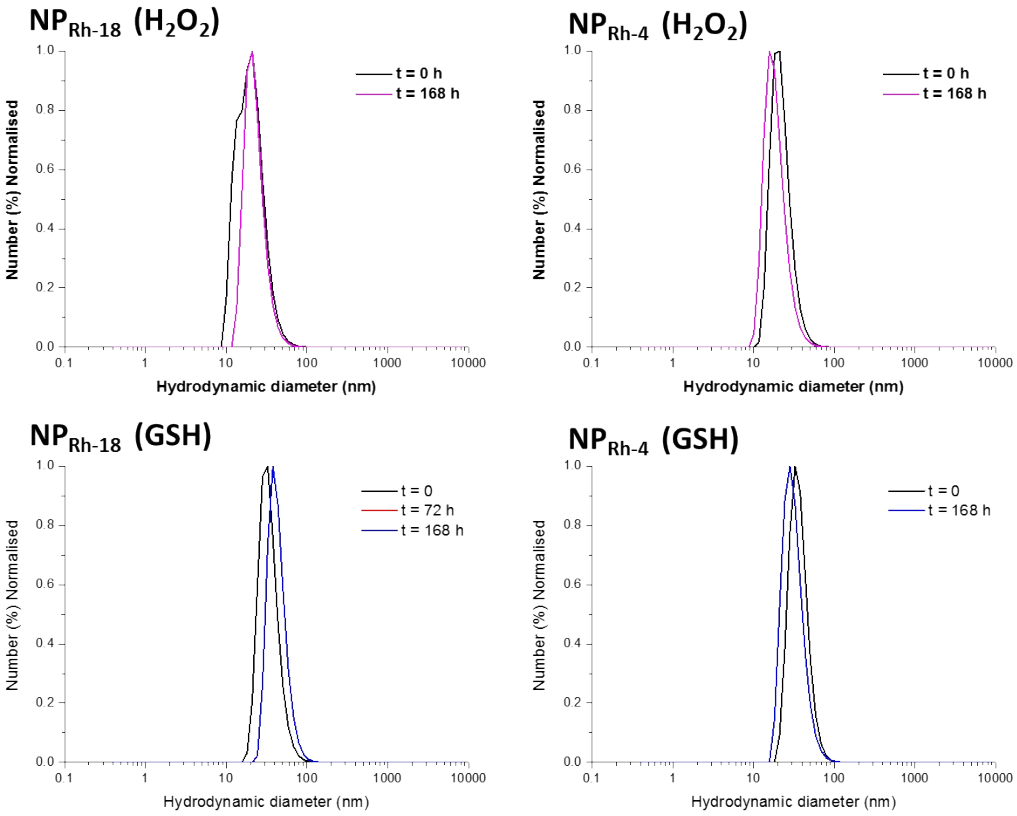

Fig. S17. Particle size distribution curves of **NP$_{Rh-n}$** (n = 4, 18) by dynamic light scattering (1 mg/mL) as function of time in aqueous H_2O_2 (5mM, top row) and GSH (5mM, bottom row)

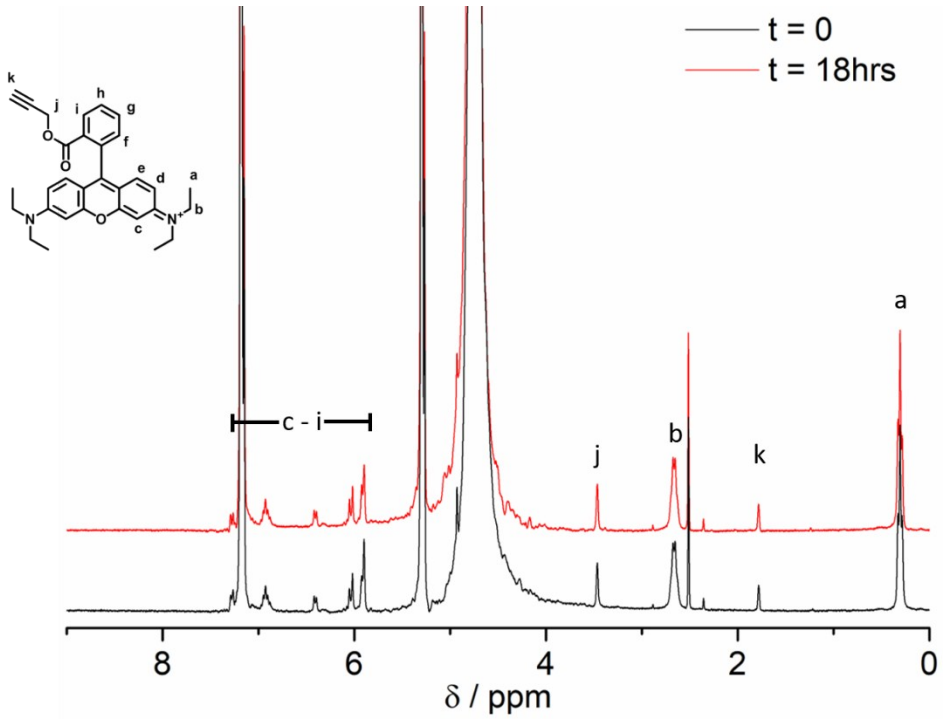

Fig. S18. ^{1}H NMR experiment (D_2O, H_3PO_2, KI, 60 °C) to investigate potential hydrolysis of propargyl-O-rhodamine B ester during cross-linking *via* RCRAC. Preservation of the methylene signal (H_j) indicate that the ester does not undergo hydrolysis under the reaction conditions.

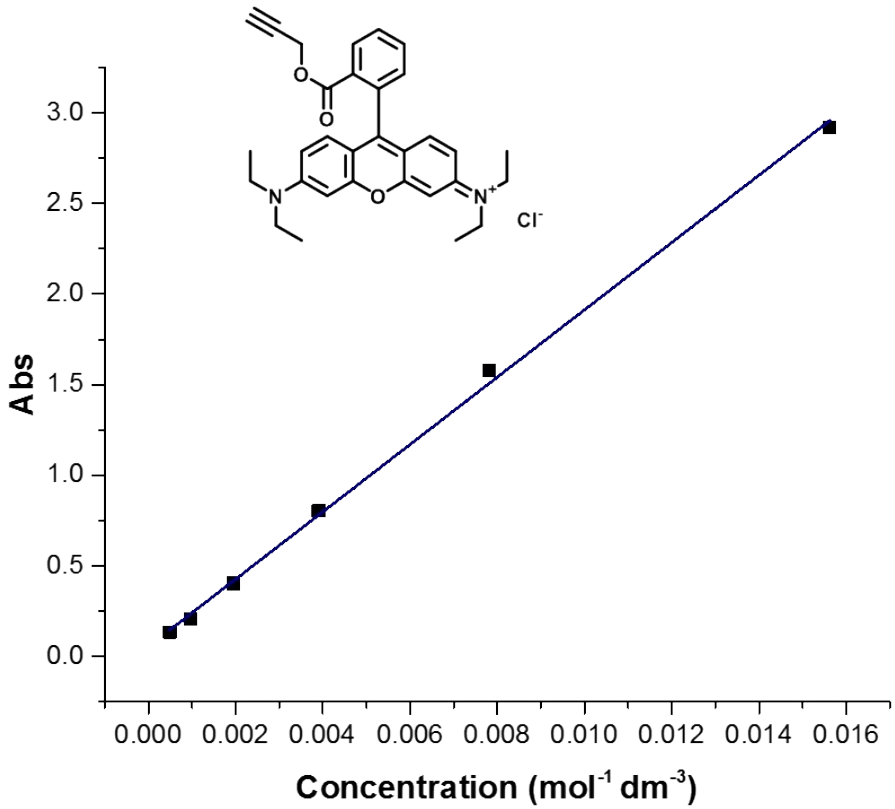

Fig. S19. UV-Vis calibration curves of propargyl-*O*-rhodamine B ester yielding theoretical crosslinking densities of $\mathbf{NP_{Rh\text{-}18}}$ = 12 %; $\mathbf{NP_{Rh\text{-}15}}$ = 12 %; $\mathbf{NP_{Rh\text{-}11}}$ = 7.1 %; $\mathbf{NP_{Rh\text{-}4}}$ = 32 %.

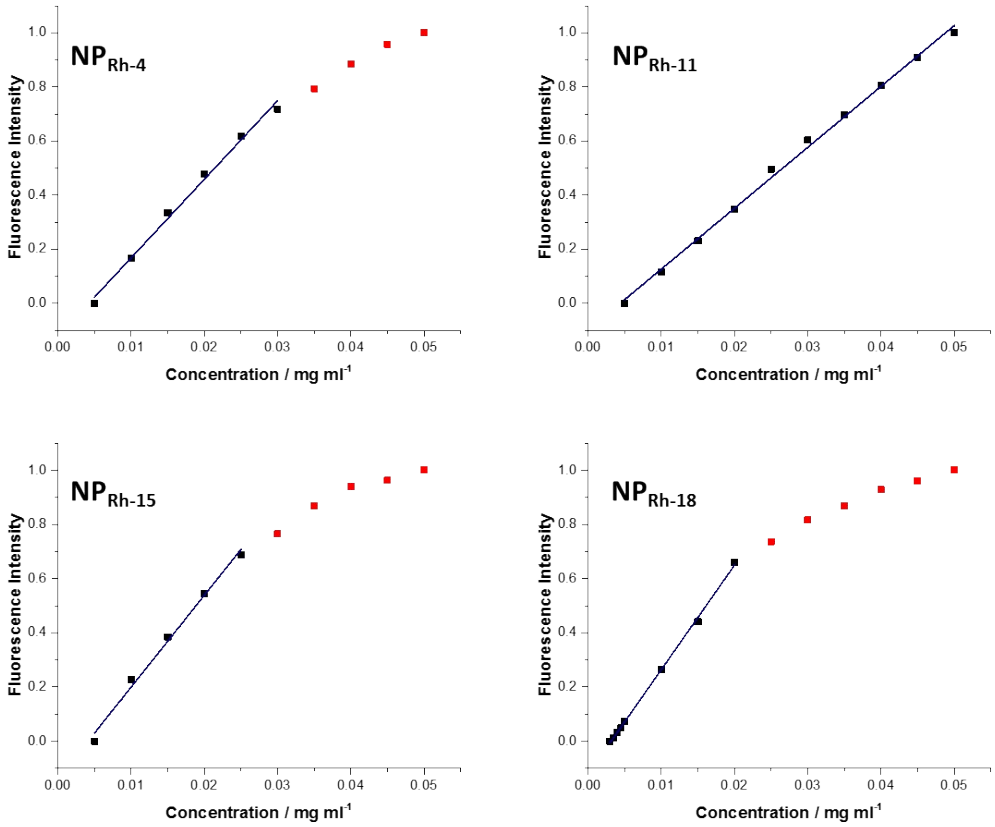

Fig. S20. Fluorescence calibration curves for $\mathbf{NP_{Rh\text{-}n}}$ (n = 4, 11, 15, 18). Concentration at the linear region was used for normalisation. At higher concentration, self-quenching of the fluorophore was observed (red dots).

Table S4. Normalisation factors calculated and applied for $\mathbf{NP_{Rh\text{-}n}}$ from the gradients of the linear regions of concentration/ fluorescence intensity curves measured from 5 – 50 µg mL-1 at the wavelengths used to monitor cellular uptake (**Fig. S20**).

	Slope	Normalisation factor
$\mathbf{NP_{Rh\text{-}4}}$	29.1	1.33
$\mathbf{NP_{Rh\text{-}11}}$	22.5	1.72
$\mathbf{NP_{Rh\text{-}15}}$	33.9	1.14
$\mathbf{NP_{Rh\text{-}18}}$	38.6	1.00

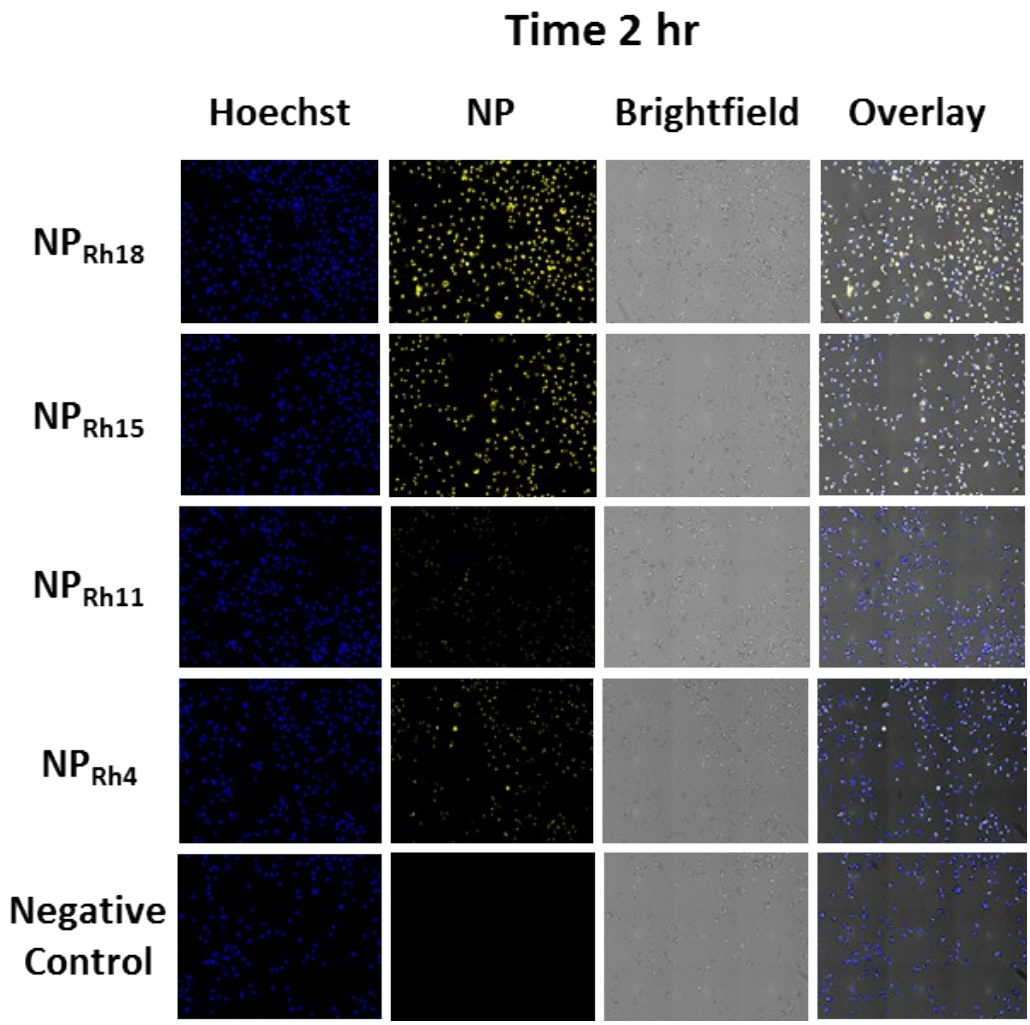

Fig. S21. Uptake of $\mathbf{NP_{Rh\text{-}n}}$ (n = 4, 11, 15 and 18) by PC3 cells after 2 hours of incubation (at 37 °C).

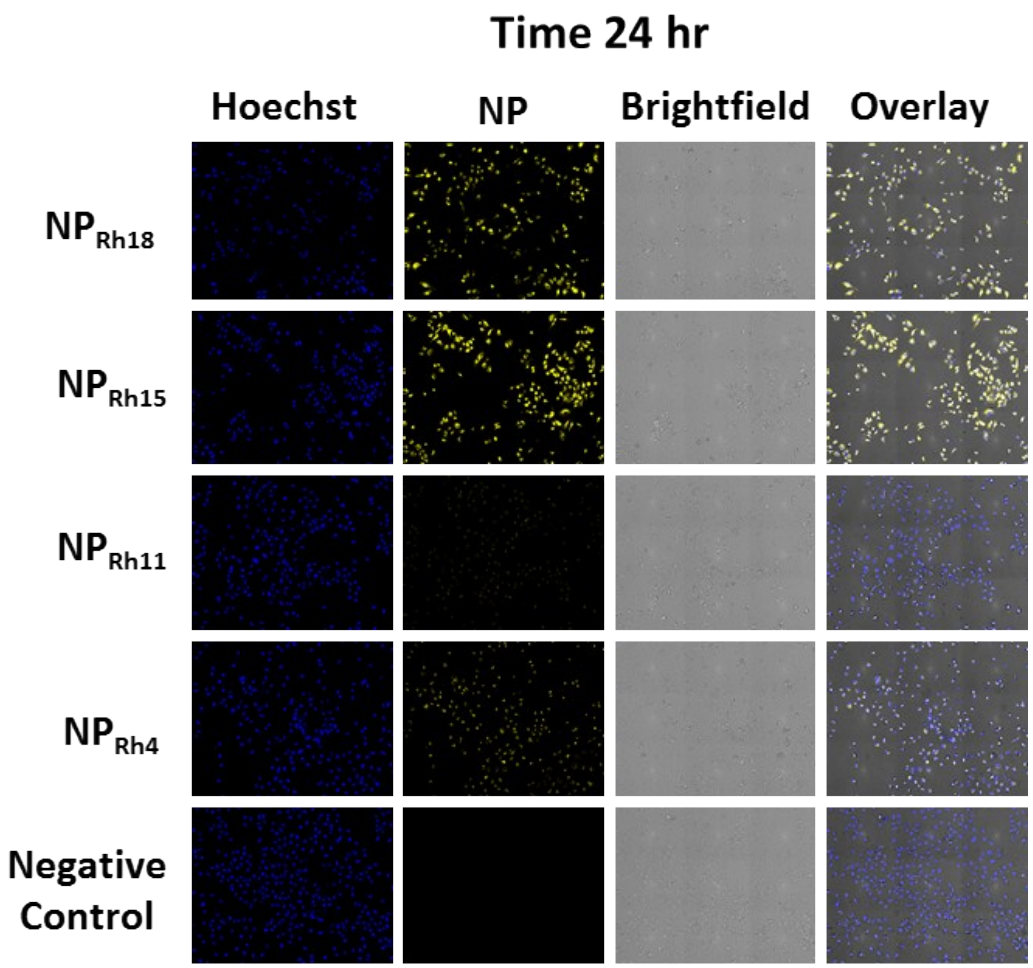

Fig. S22. Uptake of $\mathbf{NP_{Rh\text{-}n}}$ (n = 4, 11, 15 and 18) by PC3 cells after 24 hours of incubation (at 37 °C).

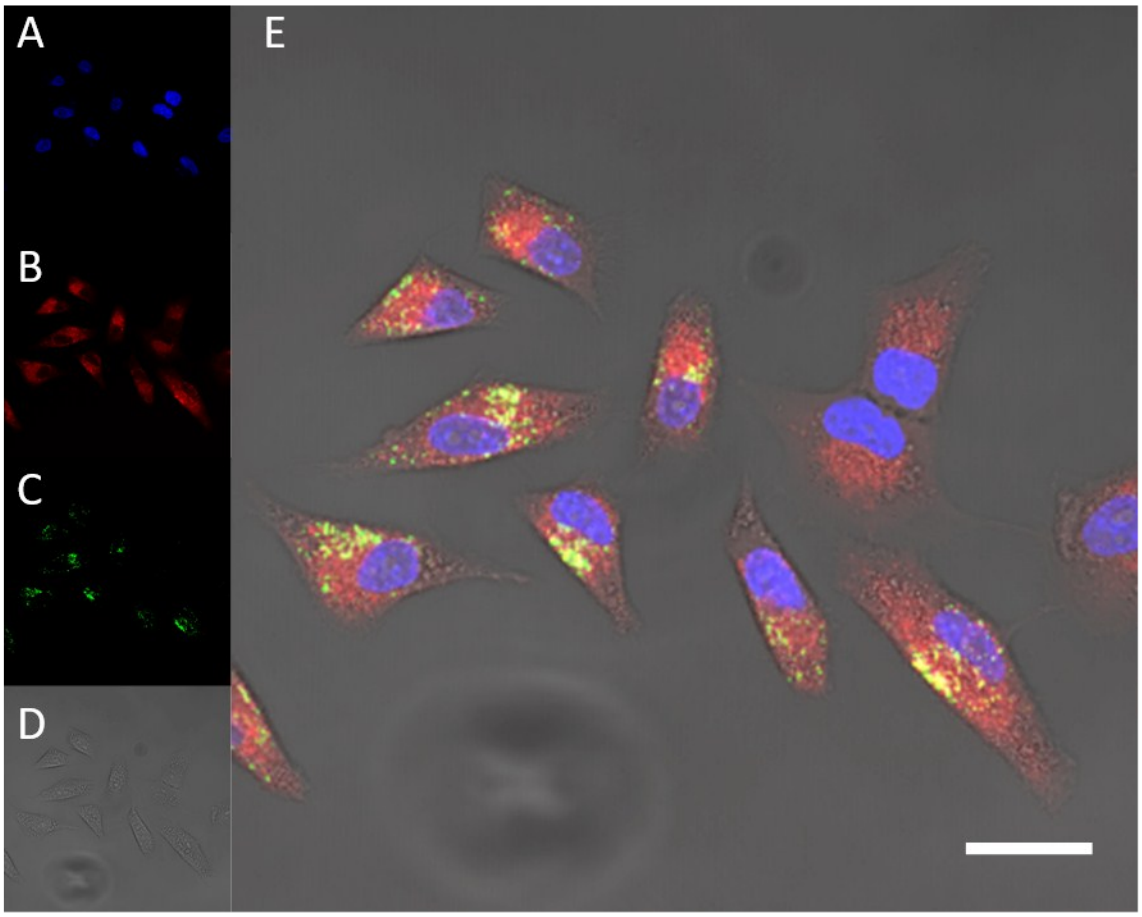

Fig. S23. Confocal fluorescent microscopy images of PC3 cells with free rhodamine B. (A) Hoechst 33258; (B) Rhodamine-B; (C) Lysotracker green; (D) Brightfield image; (E) Overlay of channels showing localisation of Rhodamine B relative to the lysosomes (scale bar = 30 μm).

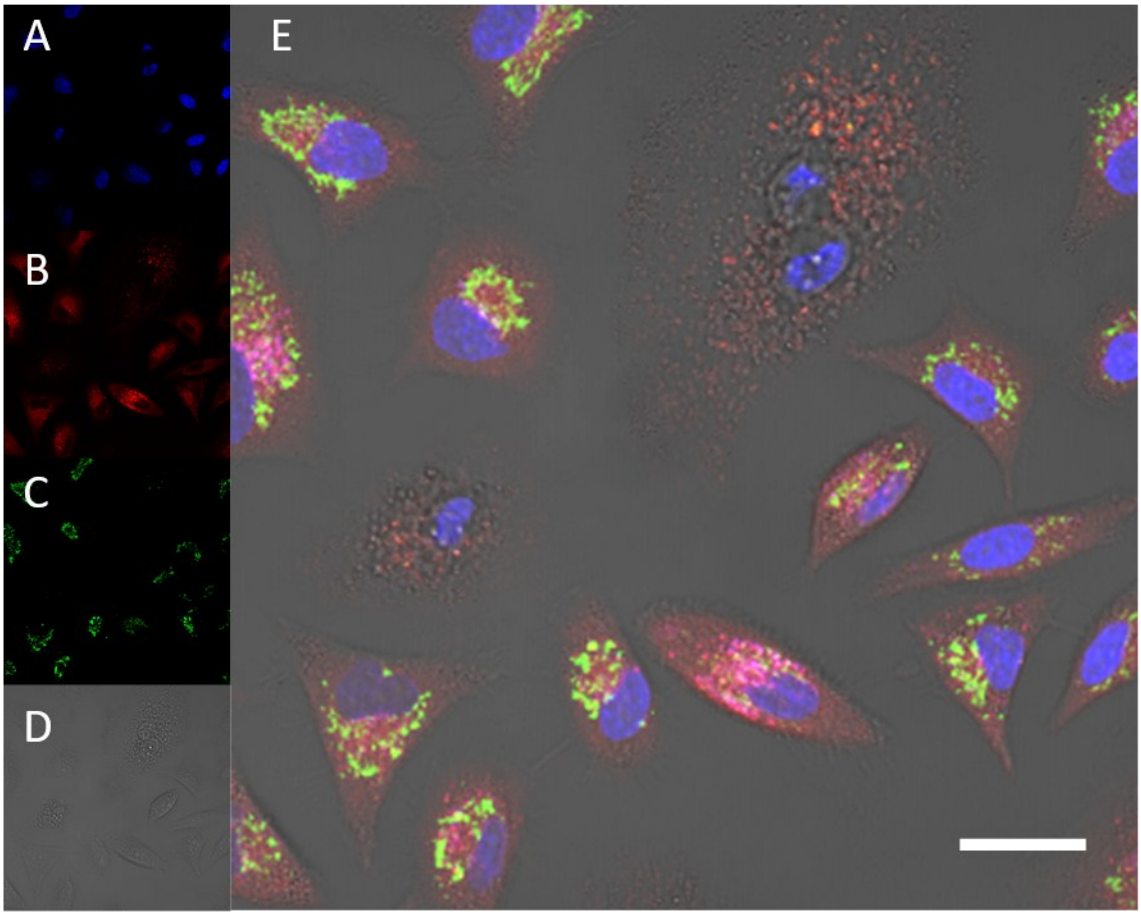

Fig. S24. Confocal fluorescent microscopy images of PC3 cells with free rhodamine B. (A) Hoechst 33258; (B) Rhodamine-B; (C) Mitotracker green; (D) Brightfield image; (E) Overlay of channels showing localisation of Rhodamine B relative to the lysosomes (scale bar = 30 μm).